Carbohydrate Polymers

Metal doped carbon nanoneedles and effect of carbon organization with activity for hydrogen evolution reaction (HER)

Rafael A. Araujo [a], Adley F. Rubira [a], Tewodros Asefa [b,c], Rafael Silva [a,*]

[a] Departamento de Química, Universidade Estadual de Maringá, Avenida Colombo 5790, CEP: 87020-900 Maringá, PR, Brazil
[b] Department of Chemistry and Chemical Biology, Rutgers, The State University of New Jersey, 610 Taylor Road, Piscataway, NJ 08854, USA
[c] Department of Chemical and Biochemical Engineering, Rutgers, The State University of New Jersey, 98 Brett Road, Piscataway, NJ 08854, USA

ARTICLE INFO

ABSTRACT

Cellulose nanowhiskers (CNW) from cotton, was prepared by acid hydrolysis and purified using a size selection process to obtain homogeneous samples with average particle size of 270 nm and 85.5% crystallinity. Purified CNW was used as precursor to carbon nanoneedles (CNN) synthesis. The synthesis of CNN loaded with different metals dopants were carried out by a nanoreactor method and the obtained CNNs applied as electrocatalysts for hydrogen evolution reaction (HER). In the carbon nanoneedles synthesis, Ni, Cu, or Fe worked as graphitization catalyst and the metal were found present as dopants in the final material. The used metal appeared to have direct influence on the degree of organization of the particles and also in the surface density of polar groups. It was evaluated the influence of the graphitic organization on the general properties and nickel was found as the more appropriate metal since it leads to a more organized material and also to a high activity toward HER.

© 2015 Elsevier Ltd. All rights reserved.

1. Introduction

The growth of world energy demand occurs while a discussion of alternatives to fossil fuels involves the scientific community. Among many options, electrochemical synthesis of chemical compounds proved to be an effective way to store energy in the most basic form of nature: the chemical bond. Hydrogen evolution reaction (HER) has been widely studied to improve water splitting technology, in which H_2 is produced from water and electricity (Lewis & Nocera, 2006). Platinum-based nanoparticles supported on carbon showed the best known catalyst activity towards HER. However, Pt cost and scantiness prevents the spread of hydrogen use on large scale as a green energy source. To address such problems, a variety of non-noble metal catalysts have been studied (Benck, Hellstern, Kibsgaard, Chakthranont, & Jaramillo, 2014; Bi, Cui, Lin, & Huang, 2015; Chao et al., 2015; Li et al., 2011b; Shervedani & Amini, 2015). In fact, the majorities of them are composed by transition metals or have transition metals in the synthesis process. The activity of transition metals on HER are already proved by nature, since Ni and Fe metal centers are the active sites of hydrogenase enzymes (Le Goff et al., 2009). Up to date, nickel (Popczun et al., 2013) or cobalt phosphide (Popczun, Read, Roske, Lewis, & Schaak, 2014) have demonstrated to provide the best known electroactivity towards HER among the non-noble metals materials. In another hand, the completion for the position of ideal catalyst for HER is still open, since phosphides have some issues regarding their syntheses. Phosphide may suffer thermal degradation releasing phosphorous, a highly corrosive and flammable specie. Therefore, phosphides syntheses must be carried out in an oxygen free environment.

Metal-free or noble metal-free electrocatalysts have brought the nanotechnology into the renewable energy sources development. Carbon based nanomaterials has been extensively applied to electrocatalysis because electronic proprieties of graphene, carbon nanotubes and nanographites (Trogadas, Fuller, & Strasser, 2014). In addition, carbon general properties allow interesting interfaces with other inorganic phases, working as catalyst supports. However, the carbon nanomaterials gained more relevance in electrocatalysis due the recent founds on intrinsic activity of heteroatom doped carbons (Liu et al., 2015; Zheng et al., 2014).

The use of nanocarbon in electrocatalysis has a very interesting aspect. Li, Tan, Lowe, Abruña, and Ralph (2011a) proved that the edge planes are 10-fold more effective on electron transfer processes than the basal planes. Sharma, Baik, Perera, and Strano (2010) and Yuan et al. (2013) also found similar results. However, the most common nanocarbons are poor regarding the content of edge planes or in some case are completely deprived of them. For instance, pristine fullerene does not possess edge planes. Carbon

* Corresponding author. Tel.: +55 44 3011 3664.
E-mail address: rsilva2@uem.br (R. Silva).

nanotubes solely present edge planes at the end of the tubes, or in the case of open end carbon nanotubes or completely free of edges planes in perfect nanotubes with two ends closed. For instance, in graphene the content of edge plane is directly correlated to the flake size, the content of edges in large graphene flakes is negligible.

As an alternative to the restricted content of edge planes in nanocarbon, carbon nanoneedles were developed by Silva, Al-Sharab, and Asefa (2012) Carbon nanoneedles are graphite nanoparticles with needle-like shape with graphitic planes oriented along the main particle axis. These nanoparticles were synthesized from cellulose nanocrystal using silica shell as template in a method known as nanoreactor. It has shown to be effective to generate carbonaceous material with high content of edge planes and also allows the doping of the particles' surface with heteroatoms, such as nitrogen, and with potential catalysts metals through a core shell intermediate therefore a prospective electrocatalysts (Silva, Pereira, Voiry, Chhowalla, & Asefa, 2015).

Cellulose nanowhiskers play an important role in the synthesis of carbon nanoneedles as the carbon source. Cellulose nanowhiskers were extensive studied because of its mechanical and chemical proprieties and as potential nanocomposites with several applications (Silva, Haraguchi, Muniz, & Rubira, 2009). They have been widely used to reinforce nano and micromaterials due fibers inherent stiffness. Nanowhiskers showed to have high crystallinity, a characteristic to be explored to produce highly ordered (low-defect) materials (Eichhorn et al., 2010). CeNW are obtained by acid hydrolysis and can be dispersed in water, methanol or ethanol. Among many cellulose sources cotton is the most used one. Therefore, CeNW synthesis is categorized as green chemistry because it uses a renewable sources and environmental friendly solvents (Nascimento et al., 2014). Different acids can be employed in this synthesis. For instance, cotton hydrolysis performed by a 65 wt.% H_2SO_4 solution for *ca* 2 h, provides nanowhiskers with average particle size in range of 200 and 400 nm (Habibi, Lucia, & Rojas, 2010).

Intrinsic activity of doped carbon nanomaterials that can perform even better than platinum in some electrochemical reactions is a remarkable but controversial subject. Most of the research works try to correlate the catalytic effect to the amount of dopants and to the chemical states of them. However, the origin and factors that affect the catalysts performed in these cases could be even more complex. The organization level of the carbonaceous materials can be one of these effects. For instance, Silva et al. in a pioneer work demonstrated that metal-free carbon nanoneedles with very well organized graphitic structure are active catalyst toward hydrazine oxidation. Recently, Meng et al. (2014) reported that the activities toward hydrazine oxidation using amorphous doped carbon are superior. Even though the carbon organization seems at a first inspection been a secondary effect, there is evidences that the degree of organization in some extensions can improve the catalytic activity of carbon materials (Banks, Crossley, Salter, Wilkins, & Compton, 2006; Silva et al., 2015). In the present work, we evaluated the effect of the carbon nanoneedles over their activity toward hydrogen evolution reaction. It is evaluated the effect of metals and other synthesis condition over general properties of CNN. Therefore, the data reported here brings insights to achieve a better understanding of how the electrocataytic activities in carbon nanomaterials are affected by their properties.

2. Experimental

2.1. Cellulose nanowhisker synthesis

CeNW were obtained by acidic hydrolysis. This method was adapted from de Oliveira Taipina, Ferrarezi, and Gonçalves (2012). First, 6 g of commercial cotton were washed with 1 M sodium hydroxide solution under stirring to remove natural oil residues. Second, cotton was thoroughly rinsed with water followed by drying in oven for 24 h at 100 °C. The fiber hydrolysis was performed with 2 g of cotton, into 40 mL of 65 wt.% sulfuric acid solution at 50 °C and under constant magnetic stirring for 2 h. Ultracentrifugation (Thermo Scientific, Sorvall Legend XTR Centrifuge) was carried out to separate acid from the cellulose nanowhiskers at 9500 rpm for 10 min. It was followed by several rinses and centrifugations of the cellulosic material to reach pH 5–6. All runs were at same speed and time.

2.2. Cellulose nanowhisker purification

A size separation was performed by ultracentrifugation in 4 steps. The first three steps (5000 rpm for 10 min; 7500 rpm for 10 min and 9500 rpm for 10 min) were planned to remove particles with size above the average particle size. In these three cases after centrifugation of dispersion the bottom part was disregarded and the stable dispersion was kept. The fourth stage was planned to remove very tiny particles, with particle size much below the average. Thus, the remained dispersion was centrifuged at 9500 rpm for 1 h, and the bottom part was kept and named as purified CeNW. The cellulosic material that has remained in the dispersion was disregarded.

2.3. Carbon nanoneedles synthesis

Six metal doped carbon nanoneedles (CNN) were synthesized. They were prepared with Cu, or Ni or Fe and treated thermally at 800 °C or 1200 °C. Purified CeNW were trapped inside a silica shell and carbonized to maintain the needle shape as described as nanoreactor method (Silva et al., 2012). In brief, the resulting amount of purified CeNW synthesized from 6.0 g of cotton was mixed with 300 mL absolute ethanol and 12 mL of distilled water in a 500 mL erlenmeyer flask under magnetic stirring for 30 min. It was added 0.1 mmol of iron(III) chloride, or copper(II) nitrate or nickel(II) nitrate under constant stirring for 30 min. Then, 5 mL of 25 wt.% ammonia solution was added. After 30 min, 1 mL of tetraethylorthosilane (TEOS) was transferred to the flask and the solution was kept under stirring for additional 24 h. The CeNW was separated from solution by centrifugation and dried in oven at 100 °C. The material was milled in a mortar and pestle prior pyrolysis in a tubular furnace at 800 °C and 1200 °C in nitrogen atmosphere.

After the pyrolysis silica was removed with a 2 M sodium hydroxide solution at 50 °C under magnetic stirring. We rinsed the particles with distilled water after centrifugations steps until neutral pH. To address metal participation on catalysis, a fraction of the 1200 °C-Ni-CNN was washed with 2 M HNO_3 solution and the sample coded was metal free-CNN.

2.4. Cellulose nanowhiskers and carbon nanoneedles characterization

CeNW were characterized by dynamic light scattering (DLS) (Particulate Systems, NanoPlus zeta/nano particle analyzer), X-ray diffraction (XRD) (X D8 Advance, Bruker), transmission electron microscope (TEM) (JEM 1400, JEOL) and thermogravimetric analyses (TGA). X-ray diffraction patterns were determined on 2θ mode, using Cu $K\alpha$ radiation, 40 kV, 35 mA and scan rate 0.5 ° min^{-1} for cotton, CeNWs and CNNs. TEM images were obtained by applying an acceleration voltage of 120 kV. A suspension containing the samples was deposited on TEM grids (carbon-Formvar-coated copper-400 mesh) and left to dry at room temperature. TGA was carried out from 30 °C to 1000 °C at heating rate of 10 °C min^{-1} under 50 ml/min N_2 flux (TGA-Q50, TA-Instruments).

The CNNs were also characterized by DLS, zeta potential, Raman spectroscopy (SENTERRA Raman microscope spectrometer, $\lambda = 785$ nm), XRD and conductivity. Conductivity was determined by resistivity measurements using a four-point probe. Electric potentials were applied on CNN pellets and current observed was measured.

2.5. Catalyst effect

The CNN prepared were tested as catalyst for HER. HER was performed under an anodic linear sweep voltammetry using a Metrohm Autolab PGSTAT302N potentiostat. A three electrodes system was used. This system was composed by saturated calomel as reference electrode, graphite rods as counter electrode and modified glassy carbon (GC) electrode as working electrode. The electrolyte solution chosen was 1 N sulfuric acid solution saturated with nitrogen.

The catalyst was applied over the surface of glassy carbon electrode as catalyst inks prepared using a propanol:water 1:3 mixture and Nafion® as binder. Inks with the six samples of CNNs prepared with Fe, Cu or Ni under 800 °C or 1200 °C pyrolysis were prepared. In order to compare the activity of the synthesized catalyst with standard system, a catalyst ink with 20% Pt/C acquired from Sigma-Aldrich was also prepared. The inks were prepared by dispersing 4 mg of dried catalyst material in a solvent mixture prepared by 0.615 mL of water in 0.205 mL of propanol with 86 µL of a 5% alcoholic solution of Nafion® purchased from Sigma-Aldrich. The mixture was kept in an ultrasonic bath for 1 h to allow complete dispersion of the particles. The electrode surface was coated by a determined volume of catalyst ink to result in 100 µg of catalyst per 1 cm² surface. Linear sweeping voltammetry was carried out from 0.2 to −1.2 V (versus SCE) using GC and RDE at 600, 800, 1200 and 1500 rpm. The current was normalized by electrode geometric area. Catalyst stability was determined by chronoamperotry at constant potential (0.8 V vs SCE) using a rotating disk electrode (RDE) for 12 h on 1500 rpm.

3. Result and discussion

In the nanoreactor method the initial shape of the cellulose nanowhiskers are explored to drive the formation of a solid silica shell that will work as a solid template in the pyrolysis stage. The silica shell shape is determined by the shape of the cellulose nanoparticle. As a consequence the quality of the cellulose nanowhiskers is a very important factor in the production of carbon nanoneedles with uniformed size and shape. In fact, different from previous works (Silva et al., 2012, 2015; Silva, Voiry, Chhowalla, & Asefa, 2013) herein we introduce a purification step based on size selection process by ultracentrifugation for the carbon nanoneedles synthesis. The evaluation of the particle size distribution was carried out by dynamic light scattering (DLS). Hydrodynamic size distribution, determined by DLS, is as reliable as particle size calculated by TEM (Varenne, Botton, Merlet, & Beck-broichsitter, 2015). DLS method takes into account the whole bulk and provides a size distribution. Antagonistically, TEM method uses only few particles depicted on the figure, therefore less statistically significant (de S. Viol, Raphael, Bettini, Ferrari, & Schiavon, 2014). In Fig. 1 it can be seen the size distribution of the cellulose nanowhiskers before and after the purification process. The prepared cellulose nanowhiskers has average particle size, by the maximum of the distribution curve at 445 nm, but a very broad distribution pattern that extend from few nanometers to few microns. It can be clearly noticed how centrifugation runs select particle size leading to narrower particle size distribution with particles size in the range from 130 to 587 nm. After purification the average size reduces to *ca.* 270 nm while
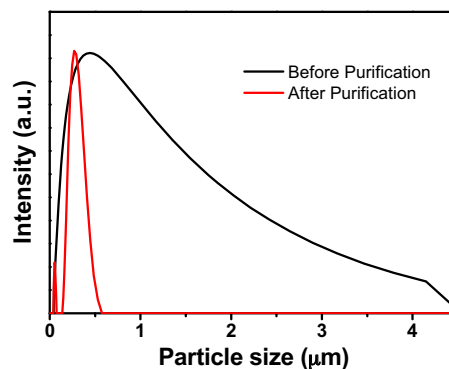

Fig. 1. Particle size distribution determined by dynamic light scattering before and after purification.

non-purified cellulosic material contained nano and microcrystalline particles.

Purified CeNW were also characterized by TEM. The morphology of particles can be observed in Fig. 2. It was possible to confirm the formation of whiskers-like particles with particle size in good agreement with DLS results. XRD pattern for cotton and purified CeNW is presented in the supplementary material in Fig S1. The degree of crystallinity of the cellulose in the cotton and in the CENWs was calculated from the XRD results. using Segal's method (Segal, Creely, & Martin, 1959) by the following equation:

$$CrI = \left(\frac{I_{22.7} - I_{18}}{I_{22.7}} \right) \times 100\% \tag{1}$$

This equation relates a peak attributed to the cellulose crystallinity at *ca* $2\theta = 22.7°$ from to the amorphous background at *ca* $2\theta = 18°$.

Cotton demonstrated to lead purified CeNW with higher crystallinity index compared to those with other carbon sources CeNW crystallinity value was determined as 85.5%, which increased from pure cotton (74.7%). The crystallinity index described in this work is higher than nanowhiskers from sugarcane bagasse (79%) (Mauricio et al., 2015) pineapple leaf fibers (73.6%), mengkuang leaves (69.5%), Avicel (81%) and wastepaper (65.8%) (Danial et al., 2015). Although the result is analogous to curaua fibers CeNW (85%) (de Oliveira Taipina et al., 2012), it is lower than Morais et al. (2013), which showed 90.45% of crystallinity index.

In Fig. 3 needle-like morphology could be noticed in CNN suggesting that silica coating prevents the structure damage during pyrolysis.

TGA analyses were made to elucidate the silica shell ability to protect purified CNW (p-CNW) during the pyrolysis leading to graphitization. It can be observed in Fig. 4 that cellulose nanoparticles not encapsulated with silica shell suffer severe degradation after *ca* 140 °C. But the sample encapsulated has a higher thermal stability, since the onset for the degradation process shift to *ca* 220 °C. A discrepancy is observed on residual mass of p-CNW and the CNW which contains cellulose nano and microcrystalline. The result suggests that impurities such as microcrystalline cellulose, carbonized particles by acid, highly sulfonated cellulose, are more resistant to thermal degradation or leads to non-volatile forms. Therefore, the purification step is shown to be effective in removing those impurities that are not essential to CNN synthesis.

Raman spectroscopy was used to investigate the structure of CNN doped with Cu, Ni and Fe. The spectra from materials are shown in Fig. 5A. It can be noticed peaks regarded to D and G bands at *ca* 1330 cm⁻¹ and *ca* 1580 cm⁻¹ respectively. Both peaks are consequence of sp² carbons. The D peak is related to breathing modes in rings and it is forbidden in perfect graphite. The G peak comes from bond stretching of sp² carbons in rings and chains. For this

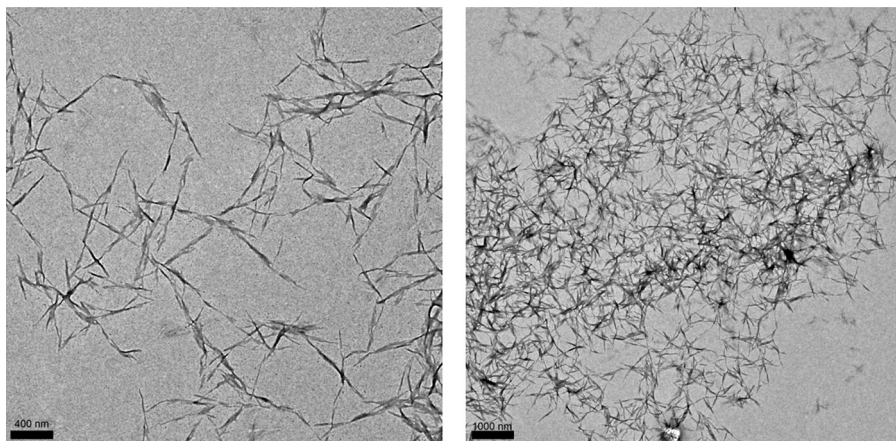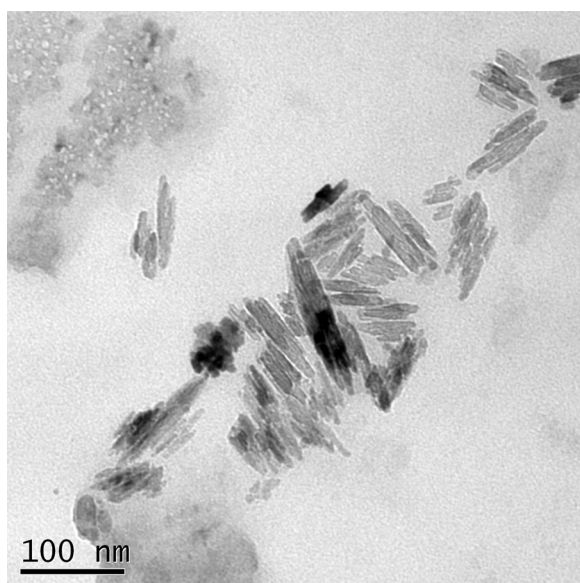**Fig. 2.** TEM images of CeNW.

Fig. 3. TEM images of CNN.

Fig. 4. Thermogravimetric curves obtained for: (a) As prepared cellulose nanowhisker (CNW), CNW after purification process, and after the encapsulation with nickel complex and silica shell; (b) purified CNW with different metals and silica shell.

reason, G bands can be related organization, but D bands to disorganization compared to bulk graphite. The I_D/I_G (D-to-G intensity ratio) values are found in Fig. 5B. They relate the ordering tendency. When I_D/I_G values are in the interval of 0.25 and 2 the structure is in a stage between graphite and nanocrystalline carbon. The G peak values are detailed in Fig. 5C. Peaks adjacent to 1580 cm^{-1} suggest a graphite structure. It is worth adding that lack of sharp second-order Raman peaks between 2400 and 3100 cm^{-1} are characteristic of amorphous carbon (Ferrari & Robertson, 2000, 2004).

The 2D band is found at 2690 cm^{-1} and is addressed to edge planes (Silva et al., 2012; Ferrari, 2007). In Fig. 5A the 2D peak is well-define for CNN-Ni but small for CNN-Fe and a bump for CNN-Cu. Nickel-CNN showed higher number of edge planes. Recognizing that Fe and Ni are known to be catalyst for graphitization in temperatures above 1000 °C (Maldonado-Hódar, Moreno-Castilla, Rivera-Utrilla, Hanzawa, & Yamada, 2000), and in addition to the results on Fig. 5A, it is suggested an amorphous form for CNN-Cu but a nanographite structure for CNN-Fe and CNN-Ni.

The XRD patterns and metals peaks are depicted in Fig. 6. Only CNN-Ni-1200 shows the graphite peak at 27.5°, as well as, nickel oxide and nickel carbide peaks. On the other hand, for the CNN-Fe-1200 and CNN-Cu-1200 the graphite peak is not present. Their structures are believed to be nanographite and amorphous
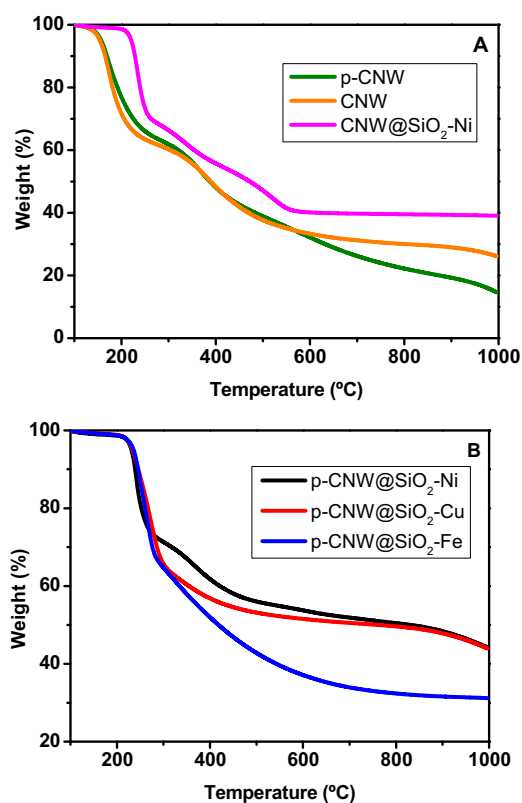
respectively, as XRD patters and Raman spectra suggest. On XRD patterns the peaks for copper oxide and iron oxide are present for each respective CNN. Their presence is believed to provide the catalyst activity to the material in a lower level than crystallinity and organized structure do.

Conductivity values were calculated as the inverse of resistivity. The resistivity values were determined using a four-point probe and calculated by Eq. (2), where V is the potential, i is the current, s the distance between the probes, B is $\pi(\ln 2)^{-1}$ and M is 1.386 (Smits, 1958; Uhlir, 1955).
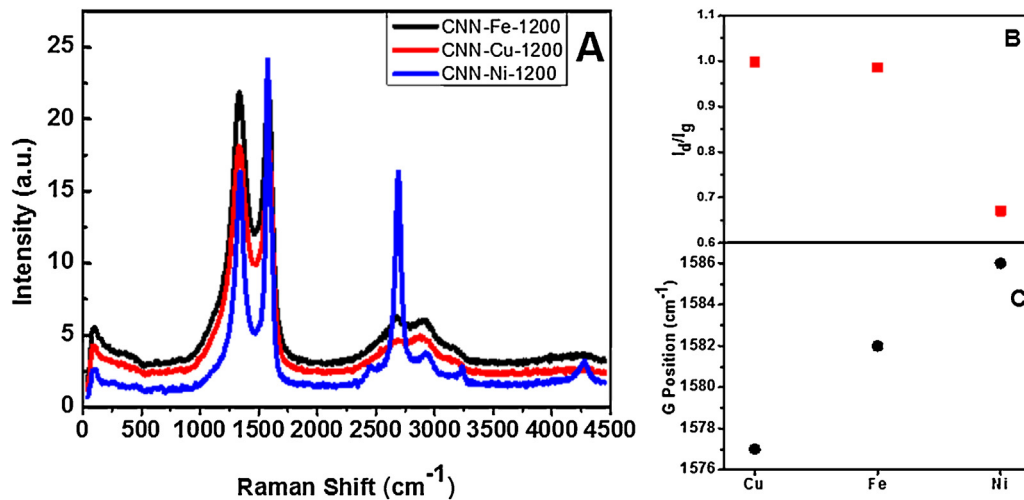
$$\rho = \frac{V}{i} s B M \qquad (2)$$

Fig. 5. (A) Raman spectra of CNN doped with 1200 °C-Ni, Cu and Fe CNN (B) I_D/I_G ratio for 1200 °C CNN (C) G band position.
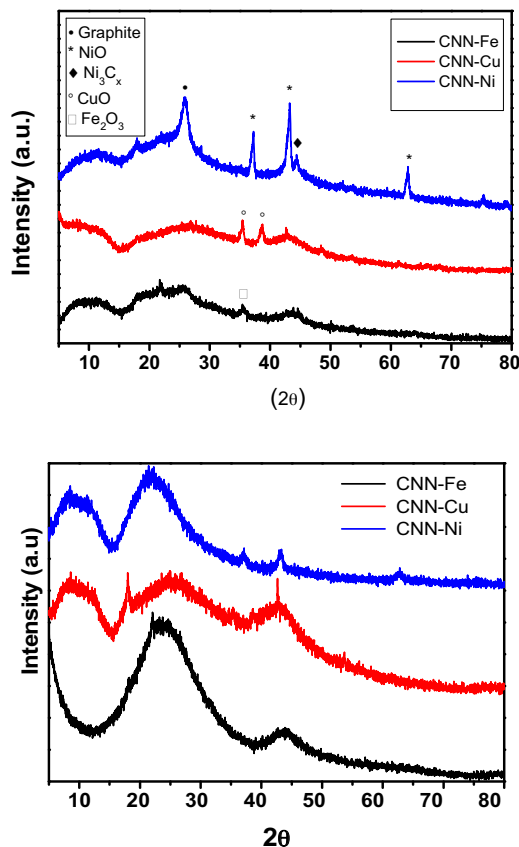

Fig. 6. XRD pattern for CNN prepared with different metal at 800 °C (top) and 1200 °C (bottom).

Table 1
Conductivity and zeta potential values for CNNs.

	Conductivity (S/m)	Zeta potential (mV)
CNN-Ni-1200	27.96 ± 0.28	−21.725 ± 0.474
CNN-Fe-1200	6.11 ± 0.10	−38.465 ± 0.403
CNN-Cu-1200	8.08 ± 0.03	−31.255 ± 1.815
CNN-Ni-800	6.47 ± 0.10	−36.97 ± 0.56
CNN-Fe-800	2.15 ± 0.06	−32.27 ± 0.83
CNN-Cu-800	15.25 ± 0.06	−40.85 ± 0.56

electronegative atoms on CNN lattice. Fe and Cu do not prevent oxygen and nitrogen to bond on carbon lattice, increasing CNN zeta potential and damaging CNN graphite structure.

Catalytic activity of the prepared samples was determined toward the hydrogen evolution reaction using Linear sweeping voltammetry (Fig. 7). In this experiment, the potential and current of hydrogen evolution is analyzed. In Fig. 7 it can be observed that bare glassy carbon electrode have poor capacity to evolve hydrogen even at very negative applied potential, HER onset for glassy carbon appears around −1.0 V vs SCE. However, it can be observed that HER occurs more easily when glassy carbon electrode is covered with a CNN, demonstrating that all CNN have activity toward HER. Among the prepared samples, CNN doped with Ni and treated at 1200 °C had the best activity. According to (Silva et al., 2012) the major effect of activity could be address to the structure and edge planes. Both degree of graphitization and durability increases with the temperature furnace applied to carbon materials
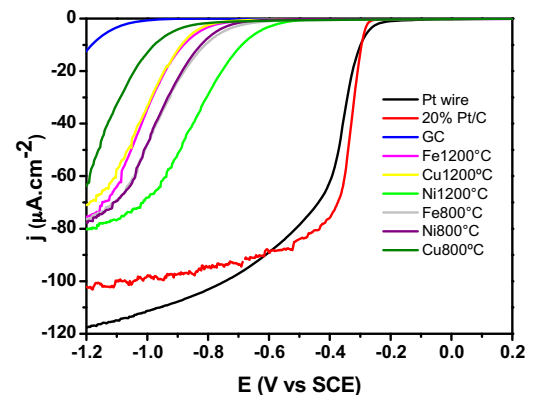
The CNN conductivity results on Table 1, corroborate the catalyst activity. The CNN-Ni-1200 has higher conductivity, therefore best material on charge transfer suggesting better catalyst activity than other CNN. Cu-CNN and Fe-CNN showed comparable activity but Cu-CNN as distinction leader. Zeta potential results contribute to address the organization and structure as major features for electrochemical activity. The negative values arise from electronegative atoms (oxygen and nitrogen) on the graphite lattice originated during pyrolysis (Krishnamoorthy, Veerapandian, Yun, & Kim, 2013). Therefore, Cu, Fe and Ni play different role in the graphitization mechanisms. Nickel generates low-defected material and due less

Fig. 7. LSV curves of CNN doped with Ni, Cu, Fe at 800 °C and 1200 °C; GC electrode; Pt wire; 20%Pt supported on carbon.

(Tsuji et al., 2015). In the case of Ni and Fe, higher activity was obtained at higher pyrolysis temperature (1200 °C). On the other hand, when Cu is used, the higher activity is observed to the sample prepared at lower pyrolysis temperature (800 °C). It is interesting since the conductivity of the sample follow the same trend. For Ni and Fe, the samples prepared at 1200 °C have higher conductivity. However, in the case of Cu higher conductivity is obtained at 800 °C. Therefore, metal dopants must play a role on carbon organization and material conductivity has direct correlation with the catalytic activity.

To further investigate the effect of the metal in the catalytic activity, a new sample was prepared by the removal of the metal from the prepared CNN. In this case CNN-Ni-1200 was subjected to mild acid treatment to promote the leaching of the metal phase from the sample. The catalytic activity of the sample after metal removal is presented in Fig. S9. After the removal of Ni the onset potential to the HER process shift ca. 0.5 V. It clearly indicate the catalytic activity of the carbonaceous materials is dependent of metal doping.

In addition, the effect of the carbon organization was verified by the preparation of CNN-Ni-1200 using unpurified cellulose, name as u-CNN-Ni-1200. A very important found is observed in the catalytic activity of u-CNN-Ni-1200 in Fig S9. The catalytic activity u-CNN-Ni-1200 is much lower than CNN-Ni-1200. So, the quality of the cellulose precursor has direct impact on the catalytic activity of the carbon nanoneedles (CNN). The onset potential to u-CNN-Ni-1200 is 0.4 V worse than CNN-Ni-1200.

The stability of the catalytic activity of than CNN-Ni-1200 was tested by chronoamperometry. In this experiment, the catalyst was used to carry out the HER for period of 12 h at constant applied potential of −0.8 V vs SCE. The result can be observed in Fig S10. It can be seen a stable current density from CNN-Ni-1200 in the first 20,000 min. After 20,000 min the current density start to slightly decrease. Importantly, after 42,000 min, the current density observed with than CNN-Ni-1200 is still around 80% of the initial current. Therefore, it can be state that after 12 h of direct use the catalyst present 80% of its catalytic activity, demonstrating than CNN-Ni-1200 is stable over a long reaction time.

4. Conclusions

The synthesis of CNW and CNN with different doped metals at two temperatures has been described. It is shown that nanowhiskers purification can be carried out by sequential centrifugation leading to particle size selection. Electrocatalytic activity of CNN-Fe, CNN-Cu and CNN-Ni were presented and CNN-Ni-1200 demonstrated to be the best catalyst for HER among all synthesized materials. Results suggest its activity is mostly due to high number of edge planes and graphite organization and in a lower level to metal dopants. Each metal is characteristic to an unknown mechanism of protection inside the silica shell preventing pyrolysis damages on graphite organization leading to different electrochemical activity. The removal of the metal by acid leaching let to severe decrease of the catalytic activity for CNN-Ni-1200. The purified CNW also has importance in the observed catalytic activity of CNN-Ni-1200, since when unpurified CNW is used the catalytic activity is much lower. CNN-Ni-1200 showed outstanding catalytic stability, retaining 80% of its catalytic activity after 12 h of direct use.

Appendix A. Supplementary data

Supplementary material related to this article can be found, in the online version, at doi:10.1016/j.carbpol.2015.11.036.

References

Banks, C. E., Crossley, A., Salter, C., Wilkins, S. J., & Compton, R. G. (2006). Carbon nanotubes contain metal impurities which are responsible for the "Electrocatalysis" seen at some nanotube-modified electrodes. Angewandte Chemie—International Edition, 45(16), 2533–2537, http://doi.org/10.1002/anie.200600033

Benck, J. D., Hellstern, T. R., Kibsgaard, J., Chakthranont, P., & Jaramillo, T. F. (2014). Catalyzing the hydrogen evolution reaction (HER) with molybdenum sulfide nanomaterials. ACS Catalysis, 4(11), 3957–3971.

Bi, H., Cui, H., Lin, T., & Huang, F. (2015). Graphene wrapped copper–nickel nanospheres on highly conductive graphene film for use as counter electrodes of dye-sensitized solar cells. Carbon, 91, 153–160, http://doi.org/10.1016/j.carbon.2015.04.051.

Chao, S., Bai, Z., Cui, Q., Yan, H., Wang, K., & Yang, L. (2015). Hollowed-out octahedral Co/N-codoped carbon as a highly efficient non-precious metal catalyst for oxygen reduction reaction. Carbon, 82, 77–86, http://doi.org/10.1016/j.carbon.2014.10.034.

Danial, W. H., Abdul Majid, Z., Mohd Muhid, M. N., Triwahyono, S., Bakar, M. B., & Ramli, Z. (2015). The reuse of wastepaper for the extraction of cellulose nanocrystals. Carbohydrate Polymers, 118, 165–169, http://doi.org/10.1016/j.carbpol.2014.10.072.

de Oliveira Taipina, M., Ferrarezi, M. M. F., & Gonçalves, M. D. C. (2012). Morphological evolution of curauá fibers under acid hydrolysis. Cellulose, 19(4), 1199–1207, http://doi.org/10.1007/s10570-012-9715-3.

de S. Viol, L. C., Raphael, E., Bettini, J., Ferrari, J. L., & Schiavon, M. A. (2014). A simple strategy to prepare colloidal Cu-doped ZnSe(S) green emitter nanocrystals in aqueous media. Particle & Particle Systems Characterization, 31(10), 1084–1090, http://doi.org/10.1002/ppsc.201300376.

Eichhorn, S. J., Dufresne, a., Aranguren, M., Marcovich, N. E., Capadona, J. R., Rowan, S. J., et al. (2010). Review: Current international research into cellulose nanofibres and nanocomposites. Journal of Materials Science, 45, http://doi.org/10.1007/s10853-009-3874-0.

Ferrari, A. C., & Robertson, J. (2000). Interpretation of Raman spectra of disordered and amorphous carbon. Physical Review B, 61(20), 14095–14107, http://doi.org/10.1103/PhysRevB.61.14095.

Ferrari, A. C., & Robertson, J. (2004). Raman spectroscopy of amorphous, nanostructured, diamond-like carbon, and nanodiamond. Philosophical Transactions Series A, Mathematical, Physical, and Engineering Sciences, 362(1824), 2477–2512, http://doi.org/10.1098/rsta.2004.1452.

Ferrari, A. C. (2007). Raman spectroscopy of graphene and graphite: Disorder, electron–phonon coupling, doping and nonadiabatic effects. Solid State Communications, 143, 47–57, http://doi.org/10.1016/j.ssc.2007.03.052.

Habibi, Y., Lucia, L. A., & Rojas, O. J. (2010). Cellulose nanocrystals: Chemistry, self-assembly, and applications. Chemical Reviews, 110(6), 3479–3500, http://doi.org/10.1021/cr900339w.

Krishnamoorthy, K., Veerapandian, M., Yun, K., & Kim, S.-J. (2013). The chemical and structural analysis of graphene oxide with different degrees of oxidation. Carbon, 53, 38–49, http://doi.org/10.1016/j.carbon.2012.10.013.

Le Goff, A., Artero, V., Jousselme, B., Tran, P. D., Guillet, N., Métayé, R., et al. (2009). From hydrogenases to noble metal-free catalytic nanomaterials for H2 production and uptake. Science, 326(December), 1384–1387, http://doi.org/10.1126/science.1179773.

Lewis, N. S., & Nocera, D. G. (2006). Powering the planet: Chemical challenges in solar energy utilization. Proceedings of the National Academy of Sciences, 103(43), 15729–15735.

Li, W., Tan, C., Lowe, M. A., Abruña, H. D., & Ralph, D. C. (2011). Electrochemistry of individual monolayer graphene sheets. ACS Nano, 5(3), 2264–2270.

Li, Y., Wang, H., Xie, L., Liang, Y., Hong, G., & Dai, H. (2011). MoS2 nanoparticles grown on graphene: An advanced catalyst for the hydrogen evolution reaction. Journal of the American Chemical Society, 133, 7296–7299.

Liu, X., Zhou, W., Yang, L., Li, L., Zhang, Z., Ke, Y., et al. (2015). Nitrogen and sulfur co-doped porous carbon derived from human hair as highly efficient metal-free electrocatalysts for hydrogen evolution reactions. Journal of Materials Chemistry A, 3(16), 8840–8846, http://doi.org/10.1039/C5TA01209K.

Maldonado-Hódar, F. J., Moreno-Castilla, C., Rivera-Utrilla, J., Hanzawa, Y., & Yamada, Y. (2000). Catalytic graphitization of carbon aerogels by transition metals. Langmuir, 16(9), 4367–4373, http://doi.org/10.1021/la991080r.

Mauricio, M. R., da Costa, P. G., Haraguchi, S. K., Guilherme, M. R., Muniz, E. C., & Rubira, A. F. (2015). Synthesis of a microhydrogel composite from cellulose nanowhiskers and starch for drug delivery. Carbohydrate Polymers, 115, 715–722, http://doi.org/10.1016/j.carbpol.2014.07.063.

Meng, Y., Voiry, D., Goswami, A., Zou, X., Huang, X., Chhowalla, M., et al. (2014). N-, O-, and S-tridoped nanoporous carbons as selective catalysts for oxygen

reduction and alcohol oxidation reactions. *Journal of the American Chemical Society*, 136(39), 13554–13557, http://doi.org/10.1021/ja507463w.

Morais, J. P. S., Rosa, M. D. F., De Souza Filho, M. D. S. M., Nascimento, L. D., Do Nascimento, D. M., & Cassales, A. R. (2013). Extraction and characterization of nanocellulose structures from raw cotton linter. *Carbohydrate Polymers*, 91(1), 229–235, http://doi.org/10.1016/j.carbpol.2012.08.010.

Nascimento, D. M., Almeida, J. S., Dias, A. F., Figueirêdo, M. C. B., Morais, J. P. S., Feitosa, J. P. A., et al. (2014). A novel green approach for the preparation of cellulose nanowhiskers from white coir. *Carbohydrate Polymers*, 110, 456–463, http://doi.org/10.1016/j.carbpol.2014.04.053.

Popczun, E. J., McKone, J. R., Read, C. G., Biacchi, A. J., Wiltrout, A. M., Lewis, N. S., et al. (2013). Nanostructured nickel phosphide as an electrocatalyst for hydrogen evolution reaction. *Journal of the American Chemical Society*, 135, 9267–9270, http://doi.org/10.1039/c4ee00957f.

Popczun, E. J., Read, C. G., Roske, C. W., Lewis, N. S., & Schaak, R. E. (2014). Highly active electrocatalysis of the hydrogen evolution reaction by cobalt phosphide nanoparticles. *Angewandte Chemie*, 126(21), 5531–5534, http://doi.org/10.1002/ange.201402646.

Segal, L., Creely, L., & Martin, A. E. (1959). An empirical method for estimating the degree of crystallinity of native cellulose using the X-ray diffractometer. *Textile Research Journal*, 29(10), 786–794.

Sharma, R., Baik, J. H., Perera, C. J., & Strano, M. S. (2010). Anomalously large reactivity of single graphene layers and edges toward electron transfer chemistries. *Nano Letters*, 10(2), 398–405, http://doi.org/10.1021/nl902741x.

Shervedani, R. K., & Amini, A. (2015). Sulfur-doped graphene as a catalyst support: Influences of carbon black and ruthenium nanoparticles on the hydrogen evolution reaction performance. *Carbon*, 93, 762–773, http://doi.org/10.1016/j.carbon.2015.05.088.

Silva, R., Haraguchi, S. K., Muniz, E. C., & Rubira, A. F. (2009). Applications of lignocellulosic fibers in polymer chemistry and in composites. *Quimica Nova*, 32, 661–671, http://doi.org/10.1590/S0100-40422009000300010.

Silva, R., Al-Sharab, J., & Asefa, T. (2012). Edge-plane-rich nitrogen-doped carbon nanoneedles and efficient metal-free electrocatalysts. *Angewandte Chemie—International Edition*, 51(29), 7171–7175, http://doi.org/10.1002/anie.201201742.

Silva, R., Voiry, D., Chhowalla, M., & Asefa, T. (2013). Efficient metal-free electrocatalysts for oxygen reduction: Polyaniline-derived N- and O-doped mesoporous carbons. *Journal of the American Chemical Society*, 135, 7823–7826.

Silva, R., Pereira, G. M., Voiry, D., Chhowalla, M., & Asefa, T. (2015). Co_3O_4 nanoparticles/cellulose nanowhiskers-derived amorphous carbon nanoneedles: sustainable materials for supercapacitors and oxygen reduction electrocatalysis. *RSC Advances*, http://doi.org/10.1039/C5RA08037A.

Smits, F. M. (1958). Measurement of sheet resistivities with the four-point probe. *Bell System Technical Journal*, 37(3), 711–718, http://doi.org/10.1002/j.1538-7305.1958.tb03883.x.

Trogadas, P., Fuller, T. F., & Strasser, P. (2014). Carbon as catalyst and support for electrochemical energy conversion. *Carbon*, 75, 5–42, http://doi.org/10.1016/j.carbon.2014.04.005.

Tsuji, E., Yamasaki, T., Aoki, Y., Park, S.-G., Shimizu, K., & Habazaki, H. (2015). Highly durable platelet carbon nanofiber-supported platinum catalysts for the oxygen reduction reaction. *Carbon*, 87, 1–9, http://doi.org/10.1016/j.carbon.2015.01.027.

Uhlir, A. (1955). The potentials of infinite systems of sources and numerical solutions of problems in semiconductor engineering. *Bell System Technical Journal*, 34(1), 105–128, http://doi.org/10.1002/j.1538-7305.1955.tb03765.x.

Varenne, F., Botton, J., Merlet, C., & Beck-broichsitter, M. (2015). Standardization and validation of a protocol of size measurements by dynamic light scattering for monodispersed stable nanomaterial characterization. *Colloids and Surfaces A: Physicochemical and Engineering Aspects*, 486, 124–138, http://doi.org/10.1016/j.colsurfa.2015.08.043.

Yuan, W., Zhou, Y., Li, Y., Li, C., Peng, H., Zhang, J., et al. (2013). The edge- and basal-plane-specific electrochemistry of a single-layer graphene sheet. *Scientific Reports*, 3, 2248, http://doi.org/10.1038/srep02248.

Zheng, Y., Jiao, Y., Li, L. H., Xing, T., Chen, Y., Jaroniec, M., et al. (2014). Toward design of synergistically active carbon-based catalysts for electrocatalytic hydrogen evolution. *ACS Nano*, 8(5), 5290–5296, http://doi.org/10.1021/nn501434a.